Frame-Theoretic Constructions of Analog Error-Correcting Codes

Ziyuan Zhu*, Changcheng Yuan†, Ron M. Roth‡, Paul H. Siegel*, Anxiao Jiang†
* Department of Electrical and Computer Engineering, University of California San Diego, La Jolla, CA, USA
† Department of Computer Science and Engineering, Texas A&M University, College Station, TX, USA
‡ Computer Science Department, Technion, Haifa, Israel
Emails: ziz050@ucsd.edu, ericycc@tamu.edu, ronny@cs.technion.ac.il, psiegel@ucsd.edu, ajiang@cse.tamu.edu

***Abstract*—Analog error-correcting codes have been proposed for analog in-memory computing on resistive crossbars, which can accelerate vector–matrix multiplication for machine learning. Unlike traditional communication or storage channels, this setting involves a mixed noise model with small perturbations and outlier errors. Although several analog code constructions have been developed, the range of available code families remains limited. This work proposes a frame-theoretic approach to analog code design. It introduces the dodecahedron code as a highly symmetric and analytically tractable geometric construction, while the same analysis method applies more broadly to a family of polygonal and polyhedral codes. Motivated by the geometric regularity of these examples, the work further introduces a code construction method using tight frames. The results show that the proposed codes provide strong error-handling capability and often achieve state-of-the-art performance.**

I. Introduction

Analog in-memory computing is a cutting-edge technology that integrates data storage and computation directly within memory cells, enabling significant acceleration of deep neural network (DNN) computations [1], [2]. The motivation for analog in-memory computing is to overcome the "von Neumann bottleneck" by avoiding the need for massive data transfers between processors and memory [3]–[5]. This approach promises substantial improvements in speed and energy efficiency by exploiting the vector–matrix multiplications within crossbar architectures [6], a fundamental operation in DNNs.

Analog error-correcting codes (analog ECCs) have been proposed to address the challenge of computing against errors [7], [8]. In this framework, redundancy is incorporated into the vector–matrix multiplication by encoding the rows of the stored matrix into codewords of a linear code over $\mathbb{R}$. By linearity, the output vector is also a codeword, and significant errors in the output can be corrected by the decoder of the code.

These codes are specifically designed to handle errors in codewords transmitted through channels that introduce two primary types of additive noise: limited-magnitude errors (LMEs) and unlimited-magnitude errors (UMEs). LMEs are small but widespread, arising from effects like cell-programming noise and random read/write disturbances in non-volatile memory (NVM) arrays. In contrast, UMEs, which arise from effects such as stuck cells or short cells, occur less frequently but can be significantly more disruptive. While DNNs can often tolerate widespread yet minor noise, they are particularly vulnerable to isolated yet large errors, making robust error correction essential for reliable in-memory computation [1].

Some existing analog ECC designs primarily aim at locating or detecting only a single UME [7], [8], while others address multiple UMEs via combinatorial code designs [9] and genetic-algorithm based code search [10]. More recently, we introduced in [11] a new class of codes whose generator matrices are designed from regular polygons and regular polyhedra, together with a linear-programming framework for analyzing their error-handling capability. These codes were presented in [11] as the duals of certain ortho-spherical parity-check (OSPC) codes, namely, codes that have a parity-check matrix whose rows are orthogonal and have the same norm, and whose columns are all unit vectors. In the language of frame theory, the column set of such a matrix forms a unit-norm tight frame [11] (see Section II below).

One of the key metrics for such codes is the m-height, which captures their error locating and detection capabilities. While [11] studied this class of codes using linear-programming and combinatorial methods, in this paper we develop an alternative geometry- and optimization-based approach for analyzing their m-height profiles. We illustrate this method for the code associated with the regular dodecahedron, while the same method can be applied more broadly to other polygonal and polyhedral codes. This approach recovers the same result as in [11]. Motivated by the geometric regularity of these codes, we then propose a frame-theoretic construction approach for analog ECC, which constructs incoherent tight frames (ITF) as its generator matrix via an alternating projection method. Results show that the proposed construction often achieves or surpasses the best known error-handling capability for a wide range of code lengths and dimensions.

II. Preliminaries

In this section, the basic definitions and notations for analog ECCs are introduced, followed by a brief review of frame-theoretic concepts that are relevant to the code constructions in this paper.

A. Height profile of analog ECC

Let $\mathcal{C}$ be a linear $[n,k]$ code over $\mathbb{R}$ (namely, a k-dimensional subspace of $\mathbb{R}^n$) that is generated by (the rows of) a real $k \times n$ matrix $G = [\boldsymbol{g}_0, \ldots, \boldsymbol{g}_{n-1}]$, where $\boldsymbol{g}_i$ is a $k \times 1$ vector. Each codeword has the form $\boldsymbol{c} = \boldsymbol{u}G$, where $\boldsymbol{u} \in \mathbb{R}^k$ is an arbitrary input vector and $\boldsymbol{c} \in \mathbb{R}^n$. For a codeword $\boldsymbol{c} = (c_0, c_1, \ldots, c_{n-1}) \in \mathcal{C}$, consider the magnitudes $|c_0|, |c_1|, \ldots, |c_{n-1}|$. Let

$$|c_{(0)}| \geq |c_{(1)}| \geq \cdots \geq |c_{(n-1)}|$$

denote the elements of $\{|c_j|\}_{j=0}^{n-1}$ sorted in nonincreasing order.

The m-height of a nonzero codeword $\boldsymbol{c}$ is defined as the ratio of its largest-magnitude entry to its $(m+1)$-th largest-magnitude entry, i.e.,

$$h_m(\boldsymbol{c}) = \frac{|c_{(0)}|}{|c_{(m)}|}.$$

If $c_{(m)} = 0$, then $h_m(\boldsymbol{c})$ is defined to be $+\infty$. The m-height of the code $\mathcal{C}$ is then

$$h_m(\mathcal{C}) = \max_{\boldsymbol{c} \in \mathcal{C} \setminus \{\boldsymbol{0}\}} h_m(\boldsymbol{c}).$$

Theorem 2 of [10] gives a general method to compute $h_m(\mathcal{C})$ by solving a family of linear programs, and a simplified version of this approach is provided in [11]. Define $[n\rangle$ as $\{0, 1, \ldots, n-1\}$. The sequence of m-heights $h_m(\mathcal{C}), m \in [n\rangle$, is called the height profile of the code $\mathcal{C}$.

B. Error model and error-handling capability of analog ECC

Let δ and Δ be positive real thresholds satisfying $\Delta > \delta > 0$. An error vector $\boldsymbol{\varepsilon} = (\varepsilon_0, \varepsilon_1, \ldots, \varepsilon_{n-1}) \in \mathbb{R}^n$ is referred to as an LME vector if $\varepsilon_i \in [-\delta, \delta]$ for all $i \in [n\rangle$. Let $\boldsymbol{e} = (e_0, e_1, \ldots, e_{n-1}) \in \mathbb{R}^n$ denote a UME vector representing outliers. A noisy received word $\boldsymbol{y} = (y_0, \ldots, y_{n-1}) \in \mathbb{R}^n$ is given by $\boldsymbol{y} = \boldsymbol{c} + \boldsymbol{\varepsilon} + \boldsymbol{e}$.

The vector $\boldsymbol{e}$ is assumed to be sparse, since it models outlier faults caused by rare events such as stuck cells or shorted cells in the array. Unlike Gaussian noise, such faults occur infrequently, but when they do occur, they typically have large magnitudes. An outlier is defined by $|e_i| > 0$. Among such outliers, **significant** outliers are those satisfying $|e_i| > \Delta$.

Following [7], [8], we define the support of an outlier vector $\boldsymbol{e}$ as

$$\mathrm{Supp}_0(\boldsymbol{e}) := \{i \in [n\rangle : |e_i| > 0\}.$$

Similarly, define the Δ-support of $\boldsymbol{e}$ as

$$\mathrm{Supp}_\Delta(\boldsymbol{e}) := \{i \in [n\rangle : |e_i| > \Delta\}.$$

The error-handling capability of analog ECC differs conceptually from that of classical error-correcting codes over finite fields because of the nature of the analog error model. For nonnegative integers τ, σ, not both zero, we say that a length-n analog code $\mathcal{C}$ is τ-error locating and $(\tau+\sigma)$-error detecting if there is a decoder

$$\mathcal{D} : \mathbb{R}^n \to \mathcal{C} \cup \{\text{“e”}\}$$

with the following property.

(i) $\mathrm{Supp}_\Delta(\boldsymbol{e}) \subseteq \mathcal{D}(\boldsymbol{y}) \subseteq \mathrm{Supp}_0(\boldsymbol{e})$, if $|\mathrm{Supp}_0(\boldsymbol{e})| \leq \tau$.
(ii) $\mathcal{D}(\boldsymbol{y})$=“e” or $\mathrm{Supp}_\Delta(\boldsymbol{e}) \subseteq \mathcal{D}(\boldsymbol{y}) \neq$ “e”, otherwise.

In other words, if $\boldsymbol{e}$ has no more than τ UMEs, the decoder output is a subset of the support of $\boldsymbol{e}$ that contains all significant UMEs. Otherwise, the decoder output is either the error flag “e” or a set of positions that includes all significant outlying errors of $\boldsymbol{e}$. Note that in the latter case, the set may include “false alarms” that are positions outside the support of $\boldsymbol{e}$.

The proof of Theorem 1 in [7], [8] introduced a particular decoder for locating τ significant UMEs and detecting $\tau + \sigma$ UMEs. Specifically, if $\boldsymbol{e}$ is a UME vector with $|\mathrm{Supp}_0(\boldsymbol{e})| \leq \tau + \sigma$, then the decoder $\mathcal{D}$ operates as follows:

(i) The output $\mathcal{D}(\boldsymbol{y})$ is “e” if there is no compatible UME vector $\boldsymbol{e}'$ such that $|\mathrm{Supp}_0(\boldsymbol{e}')| \leq \tau$.
(ii) Otherwise, the output $\mathcal{D}(\boldsymbol{y})$ is a set of size at most τ, defined as the intersection of the supports of all compatible UME vectors $\boldsymbol{e}'$ with $|\mathrm{Supp}_0(\boldsymbol{e}')| \leq \tau$. By Lemma 2 in [8], this set is guaranteed to contain $\mathrm{Supp}_\Delta(\boldsymbol{e})$.

The following example further illustrates the behavior of the decoder for the $[n,1]$ repetition code over $\mathbb{R}$ discussed in Example 1 of [8].

Example II.1. *Consider the repetition code*

$$\mathcal{C} = \{(a, a, \ldots, a) \in \mathbb{R}^{12} : a \in \mathbb{R}\},$$

with parameters

$$n = 12, \quad k = 1, \quad \delta = 1, \quad \Delta = 4, \quad \tau = 5, \quad \sigma = 1.$$

Assume that the transmitted input is $u = 0$, so the transmitted codeword is

$$\boldsymbol{c} = (0, 0, \ldots, 0).$$

The received vector is

$$\boldsymbol{y} = \boldsymbol{c} + \boldsymbol{e} + \boldsymbol{\varepsilon},$$

where $|\varepsilon_i| \leq 1$ for all $i \in [12\rangle$.

We consider the following three cases.

(i) A case with $|\mathrm{Supp}_0(\boldsymbol{e})| \leq \tau$. *Let*

$$\boldsymbol{e} = (5,\ 4.5,\ 2.6,\ 2,\ 0,\ 0,\ 0,\ 0,\ 0,\ 0,\ 0,\ 0),$$

and let $\boldsymbol{\varepsilon} = \boldsymbol{0}$. Then

$$\boldsymbol{y} = (5,\ 4.5,\ 2.6,\ 2,\ 0,\ 0,\ 0,\ 0,\ 0,\ 0,\ 0,\ 0),$$

and

$$\mathrm{Supp}_0(\boldsymbol{e}) = \{0, 1, 2, 3\}, \qquad \mathrm{Supp}_\Delta(\boldsymbol{e}) = \{0, 1\}.$$

The possible compatible codewords $\boldsymbol{c}' = (a, \ldots, a)$ with a compatible UME vector $\boldsymbol{e}'$ satisfying

$$|\mathrm{Supp}_0(\boldsymbol{e}')| \leq 5$$

are those with $a \in [-1, 1]$.

If $a \in [-1, 1)$, then

$$\mathrm{Supp}_0(\boldsymbol{e}') = \{0, 1, 2, 3\}.$$

If $a = 1$, then

$$\mathrm{Supp}_0(\boldsymbol{e}') = \{0, 1, 2\}.$$

Hence, the possible supports are

$$\{0, 1, 2, 3\} \qquad \textit{and} \qquad \{0, 1, 2\},$$

and therefore

$$\mathcal{D}(\boldsymbol{y}) = \{0, 1, 2\}.$$

***(ii) A case with** $\tau < |\mathrm{Supp}_0(\boldsymbol{e})| \le \tau + \sigma$**.** Let*

$$\boldsymbol{e} = (5,\ 5,\ 4.6,\ 4.3,\ 2.7,\ 2.4,\ 0,\ 0,\ 0,\ 0,\ 0,\ 0),$$

and let $\boldsymbol{\varepsilon} = \mathbf{0}$. Then

$$\boldsymbol{y} = (5,\ 5,\ 4.6,\ 4.3,\ 2.7,\ 2.4,\ 0,\ 0,\ 0,\ 0,\ 0,\ 0),$$

and

$$\mathrm{Supp}_0(\boldsymbol{e}) = \{0, 1, 2, 3, 4, 5\},$$

$$\mathrm{Supp}_\Delta(\boldsymbol{e}) = \{0, 1, 2, 3\}.$$

There is no compatible codeword $\boldsymbol{c}' = (a, \ldots, a)$ such that the corresponding compatible UME vector $\boldsymbol{e}'$ satisfies

$$|\mathrm{Supp}_0(\boldsymbol{e}')| \le 5.$$

Therefore,

$$\mathcal{D}(\boldsymbol{y}) = \text{“}e\text{”}.$$

***(iii) A case with** $|\mathrm{Supp}_0(\boldsymbol{e})| > \tau + \sigma$**.** Let*

$$\boldsymbol{e} = (5,\ 5,\ 5,\ 5,\ 5,\ 5,\ 5,\ 3,\ 3,\ 3,\ 3,\ 3),$$

and let $\boldsymbol{\varepsilon} = \mathbf{0}$. Then

$$\boldsymbol{y} = (5,\ 5,\ 5,\ 5,\ 5,\ 5,\ 5,\ 3,\ 3,\ 3,\ 3,\ 3),$$

and

$$|\mathrm{Supp}_0(\boldsymbol{e})| = 12 > \tau + \sigma = 6.$$

Taking

$$\boldsymbol{c}' = (4, 4, \ldots, 4),$$

we have

$$|y_i - 4| \le 1, \qquad \forall i \in [12\rangle,$$

so there exists a compatible decomposition with

$$\boldsymbol{e}' = \mathbf{0}.$$

Hence,

$$\mathcal{D}(\boldsymbol{y}) = \varnothing.$$

C. Frame-theoretic preliminaries

To understand frame-theoretic construction of analog ECCs, let us first introduce some concepts on frames. A frame is a generalization of a basis that allows for redundancy, often represented by a collection of vectors [12]. Consider the $k \times n$ matrix $G = [\boldsymbol{g}_0, \ldots, \boldsymbol{g}_{n-1}]$. From the frame-theoretic viewpoint, the columns of G form a collection of n vectors in $\mathbb{R}^k$. If the unit-norm condition

$$\|\boldsymbol{g}_i\|_2 = 1, \qquad \forall i \in [n\rangle,$$

holds, then all columns lie on the unit sphere in $\mathbb{R}^k$.

The Gram matrix is defined as the following positive semidefinite matrix [12]

$$M := G^\top G \in \mathbb{R}^{n \times n}.$$

The entries of M are given by

$$M_{ij} = \boldsymbol{g}_i \cdot \boldsymbol{g}_j = \boldsymbol{g}_i^\top \boldsymbol{g}_j,$$

so M contains all pairwise inner products among the columns of G.

A set of vectors $\{\boldsymbol{g}_i\}_{i=0}^{n-1} \subseteq \mathbb{R}^k$ is called a tight frame if the respective matrix $G = [\boldsymbol{g}_0, \ldots, \boldsymbol{g}_{n-1}]$ satisfies

$$GG^\top = aI_k,$$

where I_k is the $k \times k$ identity matrix. Thus, $\mathrm{rank}(M) = \mathrm{rank}(G) = \mathrm{rank}(GG^\top) = k$. If in addition each column vector $\boldsymbol{g}_i$ has unit norm (equivalently, $\mathrm{diag}(M) = \mathbf{1}$), then the frame is called a unit-norm tight frame (UNTF). In this case, the constant a equals n/k.

Following [11], we say that a $k \times n$ matrix G is *ortho-spherical* if its set of columns forms a UNTF. A linear $[n, k{=}n{-}r]$ code over $\mathbb{R}$ that has such a parity-check matrix H is called an *ortho-spherical parity-check* (OSPC) code. Equivalently, the columns of H form a UNTF.

A unit-norm frame $\{\boldsymbol{g}_i\}_{i=0}^{n-1}$ is called equiangular if there exists a constant $b \in [0, 1]$ such that

$$|M_{ij}| = b, \qquad \forall i \neq j.$$

A real equiangular tight frame (ETF) is a unit-norm tight frame that is also equiangular.

III. Analog Code based on Regular Dodecahedron

In this section, we introduce a code derived from a three-dimensional geometric structure: the dodecahedron. More broadly, the same geometric and optimization-based analysis can also be applied to other highly symmetric constructions, including codes whose generator matrices are obtained from regular polygons and the regular icosahedron. These analyses are provided in the extended version.

From the frame-theoretic viewpoint, this construction gives a unit-norm tight code in $\mathbb{R}^3$ with high symmetry. This code is related to $\mathcal{C}_{\mathrm{dod}}^{\perp}$, introduced in Example 6 of [11], where it was presented as the dual of an ortho-spherical parity-check (OSPC) code. By Lemma 12 of [11], the code $\mathcal{C}_{\mathrm{dod}}^{\perp}$ itself is also an OSPC code. The code we analyze differs from that

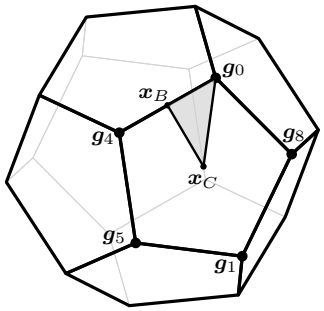

Fig. 1: Dodecahedron with a shaded triangular region indicating the fundamental search space.

construction only by permutations and sign changes of the coordinates, which do not affect the m-height profile. The dodecahedral construction is a unit-norm tight frame (UNTF) but not an equiangular tight frame (ETF).

The dodecahedron has 20 vertices, 12 faces, and 30 edges. Its 20 vertices can be grouped into 10 antipodal pairs, each pair determining a symmetric axis. For each such axis, we select one of the two corresponding vertices and denote the resulting vectors by $\{\boldsymbol{g}_0, \dots, \boldsymbol{g}_9\}$. These ten selected vertex vectors are represented by

$$G = \begin{bmatrix} 1 & 1 & 1 & 1 & 0 & 0 & \varphi^{-1} & \varphi^{-1} & \varphi & \varphi \\ 1 & 1 & -1 & -1 & \varphi & \varphi & 0 & 0 & \varphi^{-1} & -\varphi^{-1} \\ 1 & -1 & 1 & -1 & \varphi^{-1} & -\varphi^{-1} & \varphi & -\varphi & 0 & 0 \end{bmatrix}.$$

When searching for the optimal information vector $\boldsymbol{u}$ that attains the m-height, only its direction matters; that is, its magnitude does not affect the m-height. Due to the symmetry among the faces, when analyzing codewords $\boldsymbol{c} = \boldsymbol{u}G$, it suffices to consider only vectors $\boldsymbol{u}$ that point to one particular face. Moreover, that face can be divided into subregions that are symmetric to each other, so it suffices to consider only vectors $\boldsymbol{u}$ that point to one such subregion, as illustrated in Fig. 1, with vertices

$$\boldsymbol{x}_A := \boldsymbol{g}_0, \;\; \boldsymbol{x}_B := \frac{\boldsymbol{g}_0 + \boldsymbol{g}_4}{2}, \;\; \boldsymbol{x}_C := \frac{\boldsymbol{g}_0 + \boldsymbol{g}_1 + \boldsymbol{g}_4 + \boldsymbol{g}_5 + \boldsymbol{g}_8}{5}.$$

Let

$$T' = \operatorname{conv}\{\boldsymbol{x}_A, \boldsymbol{x}_B, \boldsymbol{x}_C\},$$

and

$$\boldsymbol{x}(u, v) = u\,\boldsymbol{x}_A + v\,\boldsymbol{x}_B + (1 - u - v)\,\boldsymbol{x}_C,$$

where $u, v \geq 0$ and $u + v \leq 1$. Define

$$\beta_j(\boldsymbol{x}) := |\boldsymbol{x} \cdot \boldsymbol{g}_j|.$$

Lemma III.1. *For any $\boldsymbol{x} \in T'$ we have the following inequalities:*

$$\beta_0 \geq \beta_4 \geq \beta_8 \geq \max\{\beta_5, \beta_6\}, \quad (1)$$

$$\beta_5 \geq \beta_1, \qquad \beta_5 \geq \beta_3, \qquad \beta_6 \geq \beta_3, \quad (2)$$

$$\beta_3 \geq \max\{\beta_2, \beta_7, \beta_9\}, \qquad \beta_1 \geq \max\{\beta_2, \beta_7, \beta_9\}, \quad (3)$$

$$\beta_2 \leq \beta_9. \quad (4)$$

Proof. We first compute

$$\begin{aligned}
\boldsymbol{x} \cdot \boldsymbol{g}_0 &= \Big(2 - \frac{2\sqrt{5}}{5}\Big)u + \Big(\frac{1}{2} + \frac{\sqrt{5}}{10}\Big)v + \Big(1 + \frac{2\sqrt{5}}{5}\Big), \\
\boldsymbol{x} \cdot \boldsymbol{g}_4 &= \Big(-1 + \frac{3\sqrt{5}}{5}\Big)u + \Big(\frac{1}{2} + \frac{\sqrt{5}}{10}\Big)v + \Big(1 + \frac{2\sqrt{5}}{5}\Big), \\
\boldsymbol{x} \cdot \boldsymbol{g}_8 &= \Big(-1 + \frac{3\sqrt{5}}{5}\Big)u + \Big(-\frac{1}{2} + \frac{\sqrt{5}}{10}\Big)v + \Big(1 + \frac{2\sqrt{5}}{5}\Big), \\
\boldsymbol{x} \cdot \boldsymbol{g}_1 &= \Big(-\frac{2\sqrt{5}}{5}\Big)u + \Big(-\frac{2\sqrt{5}}{5}\Big)v + \Big(1 + \frac{2\sqrt{5}}{5}\Big), \\
\boldsymbol{x} \cdot \boldsymbol{g}_5 &= \Big(-\frac{2\sqrt{5}}{5}\Big)u + \Big(-\frac{2\sqrt{5}}{5} + \frac{\sqrt{5}-1}{2}\Big)v + \Big(1 + \frac{2\sqrt{5}}{5}\Big), \\
\boldsymbol{x} \cdot \boldsymbol{g}_6 &= \Big(\frac{4\sqrt{5}}{5}\Big)u + \Big(\frac{5 + 3\sqrt{5}}{10}\Big)v + \frac{\sqrt{5}}{5}, \\
\boldsymbol{x} \cdot \boldsymbol{g}_3 &= \Big(-1 + \frac{\sqrt{5}}{5}\Big)u - \Big(\frac{1}{2} + \frac{3\sqrt{5}}{10}\Big)v - \frac{\sqrt{5}}{5}, \\
\boldsymbol{x} \cdot \boldsymbol{g}_9 &= \Big(1 - \frac{\sqrt{5}}{5}\Big)u - \frac{\sqrt{5}}{5}\,v + \frac{\sqrt{5}}{5}, \\
\boldsymbol{x} \cdot \boldsymbol{g}_2 &= \Big(1 + \frac{\sqrt{5}}{5}\Big)u + \frac{\sqrt{5}}{5}\,v - \frac{\sqrt{5}}{5}, \\
\boldsymbol{x} \cdot \boldsymbol{g}_7 &= \frac{\sqrt{5}}{5} - \Big(1 + \frac{\sqrt{5}}{5}\Big)(u + v).
\end{aligned}$$

On T', one checks that $\boldsymbol{x} \cdot \boldsymbol{g}_3 \leq 0$ everywhere, while

$$\boldsymbol{x} \cdot \boldsymbol{g}_j \geq 0 \quad \text{for } j \in \{0, 1, 4, 5, 6, 8, 9\}.$$

The only inner products that may change sign on T' are $\boldsymbol{x} \cdot \boldsymbol{g}_2$ and $\boldsymbol{x} \cdot \boldsymbol{g}_7$. Therefore, we may drop absolute values for $\boldsymbol{x} \cdot \boldsymbol{g}_j$ with $j \in \{0, 1, 4, 5, 6, 8, 9\}$, keep a minus sign for $|\boldsymbol{x} \cdot \boldsymbol{g}_3| = -(\boldsymbol{x} \cdot \boldsymbol{g}_3)$, and retain absolute values for $|\boldsymbol{x} \cdot \boldsymbol{g}_2|$ and $|\boldsymbol{x} \cdot \boldsymbol{g}_7|$.

Proof of (1). Compute the differences:

$$(\boldsymbol{x}\cdot\boldsymbol{g}_0) - (\boldsymbol{x}\cdot\boldsymbol{g}_4) = (3 - \sqrt{5})\,u \;\geq\; 0, \quad (\boldsymbol{x}\cdot\boldsymbol{g}_4) - (\boldsymbol{x}\cdot\boldsymbol{g}_8) = v \;\geq\; 0,$$

$$(\boldsymbol{x} \cdot \boldsymbol{g}_8) - (\boldsymbol{x} \cdot \boldsymbol{g}_5) = \Big(\frac{5 - \sqrt{5}}{5}\Big)u + \frac{\sqrt{5} - 1}{2}\,v \;\geq\; 0,$$

$$(\boldsymbol{x} \cdot \boldsymbol{g}_8) - (\boldsymbol{x} \cdot \boldsymbol{g}_6) = \Big(1 + \frac{\sqrt{5}}{5}\Big)\big(1 - u - v\big) \;\geq\; 0.$$

which gives $\beta_0 \geq \beta_4 \geq \beta_8 \geq \max\{\beta_5, \beta_6\}$.

Proof of (2). First,

$$(\boldsymbol{x} \cdot \boldsymbol{g}_5) - (\boldsymbol{x} \cdot \boldsymbol{g}_1) = \frac{\sqrt{5} - 1}{2}\,v \;\geq\; 0 \quad \Longrightarrow \quad \beta_5 \geq \beta_1.$$

Next,

$$\beta_5 - \beta_3 = (\boldsymbol{x}\cdot\boldsymbol{g}_5) + (\boldsymbol{x}\cdot\boldsymbol{g}_3) = 1 + \frac{\sqrt{5}}{5} - \Big(1 + \frac{\sqrt{5}}{5}\Big)(u + v) \;\geq\; 0,$$

so $\beta_5 \geq \beta_3$. Also,

$$\beta_6 - \beta_3 = (\boldsymbol{x} \cdot \boldsymbol{g}_6) + (\boldsymbol{x} \cdot \boldsymbol{g}_3) = (\sqrt{5} - 1)\,u \;\geq\; 0.$$

so $\beta_6 \geq \beta_3$.

Proof of (3). We show $|\boldsymbol{x} \cdot \boldsymbol{g}_j| \leq \beta_3$ and $|\boldsymbol{x} \cdot \boldsymbol{g}_j| \leq \beta_1$ for $j \in \{2, 7, 9\}$. For $j = 9$ (no absolute needed):

$$\beta_3 - \beta_9 = -(\boldsymbol{x} \cdot \boldsymbol{g}_3) - (\boldsymbol{x} \cdot \boldsymbol{g}_9) = \frac{1 + \sqrt{5}}{2}\,v \;\geq\; 0,$$

$$\beta_1 - \beta_9 = 1 + \frac{\sqrt{5}}{5} - \Big(1 + \frac{\sqrt{5}}{5}\Big)u - \frac{\sqrt{5}}{5}\,v \;\geq\; 0.$$

For $j = 2$, it suffices to check $\beta_3 \pm (\boldsymbol{x} \cdot \boldsymbol{g}_2) \geq 0$ and $\beta_1 \pm (\boldsymbol{x} \cdot \boldsymbol{g}_2) \geq 0$:

$$\beta_3 - (\boldsymbol{x} \cdot \boldsymbol{g}_2) = \frac{2\sqrt{5}}{5}(1-u) + \frac{5+\sqrt{5}}{10}v \;\geq\; 0,$$
$$\beta_3 + (\boldsymbol{x} \cdot \boldsymbol{g}_2) = 2u + \Big(\frac{1}{2} + \frac{\sqrt{5}}{2}\Big)v \;\geq\; 0,$$
$$\beta_1 - (\boldsymbol{x} \cdot \boldsymbol{g}_2) = 1 + \frac{3\sqrt{5}}{5} - \Big(1 + \frac{3\sqrt{5}}{5}\Big)u - \frac{3\sqrt{5}}{5}v \;\geq\; 0,$$
$$\beta_1 + (\boldsymbol{x} \cdot \boldsymbol{g}_2) = 1 + \frac{\sqrt{5}}{5} + \Big(1 - \frac{\sqrt{5}}{5}\Big)u - \frac{\sqrt{5}}{5}v \;\geq\; 0.$$

For $j = 7$, similarly check $\beta_3 \pm (\boldsymbol{x} \cdot \boldsymbol{g}_7) \geq 0$ and $\beta_1 \pm (\boldsymbol{x} \cdot \boldsymbol{g}_7) \geq 0$:

$$\beta_3 - (\boldsymbol{x} \cdot \boldsymbol{g}_7) = 2u + \Big(\frac{1}{2} + \frac{3\sqrt{5}}{10}\Big)v + \frac{\sqrt{5}}{5} \;\geq\; 0,$$
$$\beta_3 + (\boldsymbol{x} \cdot \boldsymbol{g}_7) = \frac{2\sqrt{5}}{5} - \frac{2\sqrt{5}}{5}u - \frac{5-\sqrt{5}}{10}v \;\geq\; 0,$$
$$\beta_1 - (\boldsymbol{x} \cdot \boldsymbol{g}_7) = 1 + \frac{3\sqrt{5}}{5} - \Big(1 - \frac{\sqrt{5}}{5}\Big)u - \Big(1 - \frac{3\sqrt{5}}{5}\Big)v \;\geq\; 0,$$
$$\beta_1 + (\boldsymbol{x} \cdot \boldsymbol{g}_7) = 1 + \frac{\sqrt{5}}{5} + \Big(1 + \frac{\sqrt{5}}{5}\Big)u + \frac{3\sqrt{5}}{5}v \;\geq\; 0.$$

Thus $\beta_3 \geq \max\{\beta_2, \beta_7, \beta_9\}$ and $\beta_1 \geq \max\{\beta_2, \beta_7, \beta_9\}$.

Proof of (4). Since $\beta_9 = \boldsymbol{x} \cdot \boldsymbol{g}_9 \geq 0$, it suffices to show $\beta_9 \pm (\boldsymbol{x} \cdot \boldsymbol{g}_2) \geq 0$:

$$\beta_9 - (\boldsymbol{x} \cdot \boldsymbol{g}_2) = \frac{2\sqrt{5}}{5}(1-u-v) \;\geq\; 0,$$
$$\beta_9 + (\boldsymbol{x} \cdot \boldsymbol{g}_2) = 2u \;\geq\; 0.$$

hence $|\boldsymbol{x} \cdot \boldsymbol{g}_2| \leq \boldsymbol{x} \cdot \boldsymbol{g}_9$, i.e., $\beta_2 \leq \beta_9$. □

Lemma III.2. *Let $\boldsymbol{x} \in T'$, and let $\beta_{(0)}(\boldsymbol{x}) \geq \cdots \geq \beta_{(9)}(\boldsymbol{x})$ be the elements of $\{\beta_j(\boldsymbol{x})\}_{j=0}^{9}$ sorted in non-increasing order. Under the inequalities* (1)–(4)*, the index j satisfying $\beta_j(\boldsymbol{x}) = \beta_{(\ell)}(\boldsymbol{x})$ can only belong to:*

$$\ell = 0 : \{0\}, \quad \ell = 1 : \{4\}, \quad \ell = 2 : \{8\}, \quad \ell = 3 : \{5, 6\},$$
$$\ell = 4 : \{1, 5, 6\}, \quad \ell = 5 : \{1, 3, 6\}, \quad \ell = 6 : \{1, 3\},$$
$$\ell = 7 : \{7, 9\}, \quad \ell = 8 : \{2, 7, 9\}, \quad \ell = 9 : \{2, 7\}.$$

Proof. From (1)–(4), we know that ranks $\ell = 0, 1, 2$ are attained uniquely by $\{0\}, \{4\}, \{8\}$, and the remaining ranks are determined by $\{\beta_1, \beta_2, \beta_3, \beta_5, \beta_6, \beta_7, \beta_9\}$.

From (3), we have

$$\max\{\beta_2, \beta_7, \beta_9\} \leq \min\{\beta_1, \beta_3\},$$

so $\{2, 7, 9\}$ must occupy the bottom three ranks $\ell = 7, 8, 9$, and $\{1, 3, 5, 6\}$ must occupy ranks $\ell = 3, 4, 5, 6$.

Within $\{1, 3, 5, 6\}$, inequality (2) gives

$$\beta_5 \geq \beta_1, \qquad \beta_5 \geq \beta_3, \qquad \beta_6 \geq \beta_3.$$

Hence β_1 cannot be the largest among $\{\beta_1, \beta_3, \beta_5, \beta_6\}$ since $\beta_5 \geq \beta_1$, and β_3 cannot be the largest since $\beta_5 \geq \beta_3$; therefore the largest must be attained at index 5 or 6, i.e., $\ell = 3 : \{5, 6\}$. Moreover, since both β_5 and β_6 dominate β_3, index 3 cannot be the second-largest, so the second-largest must lie in $\{1, 5, 6\}$, i.e., $\ell = 4 : \{1, 5, 6\}$. Next, because $\beta_5 \geq \beta_1$ and $\beta_5 \geq \beta_3$, index 5 cannot be the third- or fourth-largest within this subset; thus the third-largest must lie in $\{1, 3, 6\}$, i.e., $\ell = 5 : \{1, 3, 6\}$. Finally, since $\beta_6 \geq \beta_3$, index 6 cannot be the smallest among the four, so the smallest must lie in $\{1, 3\}$, i.e., $\ell = 6 : \{1, 3\}$.

Within the bottom group $\{2, 7, 9\}$, inequality (4) gives $\beta_2 \leq \beta_9$, so index 2 cannot be the largest among $\{2, 7, 9\}$ and index 9 cannot be the smallest among $\{2, 7, 9\}$. Hence

$$\ell = 7 : \{7, 9\}, \qquad \ell = 8 : \{2, 7, 9\}, \qquad \ell = 9 : \{2, 7\}.$$

□

Lemma III.3. *For each $j \in \{1, 3, 4, 5, 6, 8, 9\}$, define*

$$f_j(u, v) := \frac{\boldsymbol{x}(u, v) \cdot \boldsymbol{g}_0}{|\boldsymbol{x}(u, v) \cdot \boldsymbol{g}_j|}, \qquad \boldsymbol{x}(u, v) \in T'.$$

Then f_j has no stationary point in T'. In fact, on T' we have

$$\partial_u f_1 > 0, \quad \partial_v f_1 > 0, \qquad \partial_u f_4 > 0, \quad \partial_v f_4 \leq 0,$$
$$\partial_u f_5 > 0, \quad \partial_v f_5 > 0, \qquad \partial_u f_6 < 0, \quad \partial_v f_6 < 0,$$
$$\partial_u f_8 > 0, \quad \partial_v f_8 > 0, \qquad \partial_u f_9 < 0, \quad \partial_v f_9 > 0,$$

and for $j = 3$, $\partial_v f_3 < 0$.

Proof. On T', we have $\boldsymbol{x} \cdot \boldsymbol{g}_3 < 0$ and $\boldsymbol{x} \cdot \boldsymbol{g}_j > 0$ for $j \in \{1, 4, 5, 6, 8, 9\}$. Hence

$$|\boldsymbol{x} \cdot \boldsymbol{g}_3| = -(\boldsymbol{x} \cdot \boldsymbol{g}_3), \qquad |\boldsymbol{x} \cdot \boldsymbol{g}_j| = \boldsymbol{x} \cdot \boldsymbol{g}_j \quad j \in \{1, 4, 5, 6, 8, 9\}.$$

Write

$$N := \boldsymbol{x} \cdot \boldsymbol{g}_0 = a_0 u + b_0 v + c_0, \qquad D_j := |\boldsymbol{x} \cdot \boldsymbol{g}_j| = a_j u + b_j v + c_j.$$

Then

$$\partial_u f_j = \frac{a_0 D_j - a_j N}{D_j^2}, \qquad \partial_v f_j = \frac{b_0 D_j - b_j N}{D_j^2}.$$

Substituting the explicit formulas of $\boldsymbol{x} \cdot \boldsymbol{g}_0$ and $\boldsymbol{x} \cdot \boldsymbol{g}_j$ gives

$$\partial_u f_1 = \frac{(10 + 4\sqrt{5}) + (5 - 3\sqrt{5})v}{5D_1^2} > 0,$$
$$\partial_v f_1 = \frac{(15 + 7\sqrt{5}) + (-10 + 6\sqrt{5})u}{10D_1^2} > 0,$$
$$\partial_u f_4 = \frac{(5 + \sqrt{5}) + (5 - \sqrt{5})v}{5D_4^2} > 0,$$
$$\partial_v f_4 = \frac{(\sqrt{5} - 5)u}{5D_4^2} \leq 0,$$
$$\partial_u f_5 = \frac{(10 + 4\sqrt{5}) + (-5 + 3\sqrt{5})v}{5D_5^2} > 0,$$
$$\partial_v f_5 = \frac{(5 + 2\sqrt{5}) + (5 - 3\sqrt{5})u}{5D_5^2} > 0,$$
$$\partial_u f_6 = -\frac{2(5 + \sqrt{5})}{5D_6^2} < 0,$$
$$\partial_v f_6 = -\frac{5 + 2\sqrt{5}}{5D_6^2} < 0,$$

$$\partial_u f_8 = \frac{(5+\sqrt{5}) + (-5+\sqrt{5})v}{5D_8^2} > 0,$$
$$\partial_v f_8 = \frac{(5+2\sqrt{5}) + (5-\sqrt{5})u}{5D_8^2} > 0,$$
$$\partial_u f_9 = -\frac{(5-\sqrt{5}) + 2\sqrt{5}\,v}{5D_9^2} < 0,$$
$$\partial_v f_9 = \frac{(5+3\sqrt{5}) + 4\sqrt{5}\,u}{10D_9^2} > 0.$$

For $j = 3$, we use

$$D_3 = |\boldsymbol{x}\cdot\boldsymbol{g}_3| = -(\boldsymbol{x}\cdot\boldsymbol{g}_3)$$
$$= \Big(1 - \frac{\sqrt{5}}{5}\Big)u + \Big(\frac{1}{2} + \frac{3\sqrt{5}}{10}\Big)v + \frac{\sqrt{5}}{5},$$

and obtain

$$\partial_v f_3 = -\frac{2\sqrt{5}\,u + (5+2\sqrt{5})}{5D_3^2} < 0.$$

In each case, ∇f_j cannot be zero on T', so f_j has no stationary point in T'. □

Theorem III.4. *For each $1 \le m \le 7$, any maximizer of the corresponding m-height over T' must lie in the candidate set*

$$\mathcal{S} = \big\{(u,v) \in T' :\ (1,0),\ (0,0),\ (0,1),$$
$$\big(0, \tfrac{1+3\sqrt{5}}{11}\big),\ \big(\tfrac{\varphi}{3}, 0\big),\ \big(0, 2\sqrt{5}-4\big)\big\}.$$

Proof. We treat the cases $m = 1$, $m = 2$, $m \in \{3,4\}$, $m \in \{5,6\}$, and $m = 7$ separately.

Case $m = 1$. From Lemma III.3, we have

$$\partial_u f_4(u,v) > 0, \qquad \partial_v f_4(u,v) < 0.$$

Hence f_4 is increasing in u and decreasing in v on T', so the maximizer is attained at $(u,v) = (1,0)$, i.e., $\boldsymbol{x} = \boldsymbol{x}_A = \boldsymbol{g}_0$. Evaluating gives

$$f_4(\boldsymbol{g}_0) = \frac{\boldsymbol{g}_0\cdot\boldsymbol{g}_0}{\boldsymbol{g}_0\cdot\boldsymbol{g}_4} = \frac{3}{\sqrt{5}}.$$

Case $m = 2$. We have

$$\partial_u f_8(u,v) > 0, \qquad \partial_v f_8(u,v) > 0.$$

Thus f_8 is increasing in both u and v, and by monotonicity the maximizer lies on the edge $u + v = 1$. Along this edge,

$$f_8(u, 1-u) = \frac{(3-\sqrt{5})u + (3+\sqrt{5})}{(\sqrt{5}-1)u + (1+\sqrt{5})}$$

is strictly decreasing in u, so the unique maximizer is $(u,v) = (0,1)$, i.e., $\boldsymbol{x} = \boldsymbol{x}_B = \frac{\boldsymbol{g}_0+\boldsymbol{g}_4}{2}$. Evaluating gives

$$f_8(\boldsymbol{x}_B) = \frac{\boldsymbol{x}_B\cdot\boldsymbol{g}_0}{\boldsymbol{x}_B\cdot\boldsymbol{g}_8} = \varphi.$$

Case $m = 3, 4$ (the denominator is in $\{\boldsymbol{g}_1, \boldsymbol{g}_5, \boldsymbol{g}_6\}$). By Lemma III.2, for $m = 3, 4$, the $(m+1)$-th largest projection must be attained at index 1, 5, or 6.

Define

$$L_{i,j} := \{\boldsymbol{x} \in T' :\ |\boldsymbol{x}\cdot\boldsymbol{g}_i| = |\boldsymbol{x}\cdot\boldsymbol{g}_j|\}.$$

Since $\boldsymbol{x}\cdot\boldsymbol{g}_1,\ \boldsymbol{x}\cdot\boldsymbol{g}_5,\ \boldsymbol{x}\cdot\boldsymbol{g}_6 \ge 0$ on T', we drop the absolute values and write $L_{i,j} = \{\boldsymbol{x} \in T' : \boldsymbol{x}\cdot\boldsymbol{g}_i = \boldsymbol{x}\cdot\boldsymbol{g}_j\}$ for $i, j \in \{1,5,6\}$. The switching boundaries among these three denominators are given by

$$L_{1,6} : \boldsymbol{x}\cdot\boldsymbol{g}_1 = \boldsymbol{x}\cdot\boldsymbol{g}_6 \iff 12\sqrt{5}\,u + (7\sqrt{5}+5)\,v$$
$$= 10 + 2\sqrt{5},$$
$$L_{5,6} : \boldsymbol{x}\cdot\boldsymbol{g}_5 = \boldsymbol{x}\cdot\boldsymbol{g}_6 \iff 6\sqrt{5}\,u + (5+\sqrt{5})\,v = 5 + \sqrt{5}.$$

We do not need to consider the switching boundary $L_{1,5}$ since by Lemma III.1, $\boldsymbol{x}\cdot\boldsymbol{g}_5 \ge \boldsymbol{x}\cdot\boldsymbol{g}_1$.

By Lemma III.3, none of f_1, f_5, or f_6 has a stationary point in T'. The switching boundaries partition T' into three subregions, as illustrated in Fig. 2. Within each subregion, the ordering among the denominators is fixed, and the relevant denominator is $\boldsymbol{g}_j$ for some $j \in \{1,5,6\}$. Consequently, the m-height optimization reduces to maximizing a single ratio $f_j(u,v)$ over that subregion. We thus analyze the three subregions separately, maximizing $f_1(u,v)$, $f_5(u,v)$, or $f_6(u,v)$ on the corresponding region.

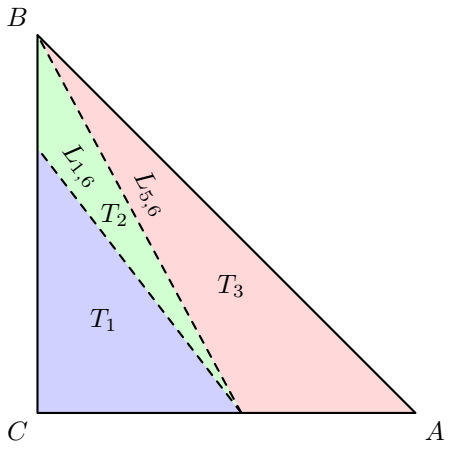

Fig. 2: Triangle T' in (u,v)-coordinates and switching lines $L_{1,6}$ and $L_{5,6}$, partitioning T' into three subregions.

(A) Maximizers in T_1. From Lemma III.3, both $\partial_u f_1$ and $\partial_v f_1$ are strictly positive. Hence f_1 is strictly increasing in both u and v, and its maximum over T_1 must be attained on the edge $L_{1,6}$. Evaluating f_1 along this edge shows that

$$f_1\Big(u, \frac{10+2\sqrt{5}-12\sqrt{5}\,u}{7\sqrt{5}+5}\Big) = \frac{(13-5\sqrt{5})u + (13+6\sqrt{5})}{(4\sqrt{5}-6)u + (5+4\sqrt{5})},$$

with derivative

$$\frac{d}{du}(\cdot) = \frac{11(\sqrt{5}-7)}{\big((4\sqrt{5}-6)u + (5+4\sqrt{5})\big)^2} < 0.$$

Hence the maximum is attained at $u = 0$, i.e.,

$$(u,v) = \Big(0,\ \frac{1+3\sqrt{5}}{11}\Big).$$

For f_5, both $\partial_u f_5$ and $\partial_v f_5$ are strictly positive. Evaluating f_5 along $L_{1,6}$ shows that

$$f_5\big(u, v(u)\big) = \frac{(6\sqrt{5}-10)u + (25+11\sqrt{5})}{(4\sqrt{5}-20)u + (15+9\sqrt{5})}.$$

Differentiating yields

$$\frac{d}{du} f_5\big(u, v(u)\big) = \frac{40(10+3\sqrt{5})}{\big((4\sqrt{5}-20)u + (15+9\sqrt{5})\big)^2} > 0.$$

Hence f_5 is strictly increasing along $L_{1,6}$ inside T', so its maximum on this segment is attained at the endpoint with largest u, namely where $v = 0$:

$$(u, v) = \Big(\frac{10+2\sqrt{5}}{12\sqrt{5}},\, 0\Big) = \Big(\frac{1+\sqrt{5}}{6},\, 0\Big).$$

For f_6, both partial derivatives satisfy $\partial_u f_6 < 0$ and $\partial_v f_6 < 0$ on T', so f_6 is strictly decreasing in both variables. Hence its maximum over T_1 is attained at the vertex $(u, v) = (0, 0)$.

(B) Maximizers in T_2. For f_1, both $\partial_u f_1$ and $\partial_v f_1$ are strictly positive. Evaluating f_1 along $L_{5,6}$ shows that

$$f_1\Big(u,\ 1 + \tfrac{3}{2}(1-\sqrt{5})u\Big) = \frac{(4-2\sqrt{5})u + (3+\sqrt{5})}{2\big((3-\sqrt{5})u + 1\big)}.$$

Differentiating gives

$$\frac{d}{du}(\cdot) = \frac{-4\sqrt{5}}{\big(2((3-\sqrt{5})u+1)\big)^2} < 0,$$

hence the maximum is attained at $u = 0$, i.e., at $(u, v) = (0, 1)$.

For f_5, both $\partial_u f_5$ and $\partial_v f_5$ are strictly positive. Evaluating f_5 along $L_{5,6}$ shows that

$$f_5\Big(u,\ 1 + \tfrac{3}{2}(1-\sqrt{5})u\Big) = \frac{(4-2\sqrt{5})u + (3+\sqrt{5})}{(\sqrt{5}-3)u + (1+\sqrt{5})}.$$

with derivative

$$\frac{d}{du}(\cdot) = \frac{10(1+\sqrt{5})}{\big((\sqrt{5}-3)u + (1+\sqrt{5})\big)^2} > 0.$$

Thus the maximum on $L_{5,6}$ is attained at the largest feasible u, which occurs at $v = 0$, i.e.,

$$(u, v) = \Big(\frac{1+\sqrt{5}}{6},\ 0\Big).$$

For f_6, both $\partial_u f_6$ and $\partial_v f_6$ are strictly negative. Evaluating f_6 along $L_{1,6}$ shows that

$$f_6\Big(u, \frac{10+2\sqrt{5}-12\sqrt{5}\,u}{7\sqrt{5}+5}\Big) = \frac{(6\sqrt{5}-10)u + (25+11\sqrt{5})}{(10-2\sqrt{5})u + (15+5\sqrt{5})}.$$

Its derivative is

$$\frac{d}{du}(\cdot) = -\frac{20(7+\sqrt{5})}{\big((10-2\sqrt{5})u + (15+5\sqrt{5})\big)^2} < 0.$$

Hence the maximum on this segment is attained at the endpoint with smallest u, i.e.,

$$(u, v) = \Big(0,\ \frac{1+3\sqrt{5}}{11}\Big).$$

(C) Maximizers in T_3. For f_1, both $\partial_u f_1$ and $\partial_v f_1$ are strictly positive. Evaluating f_1 along edge AB shows that

$$f_1(u, 1-u) = (\frac{3}{2} - \frac{\sqrt{5}}{2})u + (\frac{3}{2} + \frac{\sqrt{5}}{2}).$$

Differentiating yields

$$\frac{d}{du}(\cdot) = \frac{3}{2} - \frac{\sqrt{5}}{2} > 0,$$

so f_1 is strictly increasing along AB. Hence the maximum on AB is attained at $u = 1$, i.e., at the vertex $A = (1, 0)$.

For f_5, both $\partial_u f_5$ and $\partial_v f_5$ are strictly positive. Evaluating f_5 along edge AB shows that

$$f_5(u, 1-u) = \frac{(3-\sqrt{5})u + (3+\sqrt{5})}{(1-\sqrt{5})u + (1+\sqrt{5})}.$$

Its derivative is

$$\frac{d}{du} f_5(u, 1-u) = \frac{4\sqrt{5}}{\big((1-\sqrt{5})u + (1+\sqrt{5})\big)^2} > 0,$$

so $f_5(u, 1-u)$ is strictly increasing on u. Therefore the maximum on edge AB is attained at $u = 1$.

For f_6, both $\partial_u f_6$ and $\partial_v f_6$ are strictly negative. Evaluating f_6 along edge $L_{5,6}$ shows that

$$f_6\Big(u,\ 1 + \tfrac{3}{2}(1-\sqrt{5})u\Big) = \frac{(2-\sqrt{5})u + \frac{3+\sqrt{5}}{2}}{\frac{\sqrt{5}-3}{2}\,u + \frac{1+\sqrt{5}}{2}}.$$

Its derivative is

$$\frac{d}{du} f_6\Big(u,\ 1 + \tfrac{3}{2}(1-\sqrt{5})u\Big) = \frac{\frac{\sqrt{5}-1}{2}}{\big(\frac{\sqrt{5}-3}{2}\,u + \frac{1+\sqrt{5}}{2}\big)^2} > 0.$$

so f_6 is strictly increasing along $L_{5,6}$. Therefore, the maximum on this segment is attained at the endpoint with largest u, namely

$$(u, v) = \Big(\frac{1+\sqrt{5}}{6},\, 0\Big).$$

Case $m = 5, 6$ (the denominator is in $\{\boldsymbol{g}_1, \boldsymbol{g}_3, \boldsymbol{g}_6\}$). For $m = 5$ or $m = 6$, the $(m+1)$-th largest magnitude must be attained at index 1, 3, or 6. On T', $\boldsymbol{x}\cdot\boldsymbol{g}_1 \geq 0$ and $\boldsymbol{x}\cdot\boldsymbol{g}_6 \geq 0$, while $\boldsymbol{x}\cdot\boldsymbol{g}_3 < 0$, so $|\boldsymbol{x}\cdot\boldsymbol{g}_1| = \boldsymbol{x}\cdot\boldsymbol{g}_1$, $|\boldsymbol{x}\cdot\boldsymbol{g}_6| = \boldsymbol{x}\cdot\boldsymbol{g}_6$, and $|\boldsymbol{x}\cdot\boldsymbol{g}_3| = -(\boldsymbol{x}\cdot\boldsymbol{g}_3)$. The switching interfaces are

$$L_{1,3} : 2(5+\sqrt{5})\,u + (5+7\sqrt{5})\,v = 10 + 2\sqrt{5},$$
$$L_{1,6} : 12\sqrt{5}\,u + (7\sqrt{5}+5)\,v = 10 + 2\sqrt{5}.$$

Similar to the previous case, these lines partition T' into three subregions.

(A) Maximizers in T_1. Maximizing f_2 and f_7 in T_1 is already done in case I, thus we skip them.

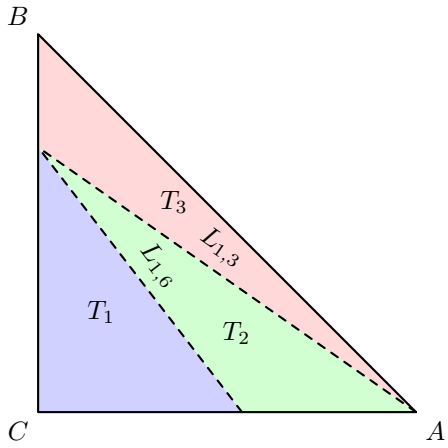

Fig. 3: Triangle T' in (u, v)-coordinates and switching lines $L_{1,3}$ and $L_{1,6}$, partitioning T' into three subregions.

For f_4, From Lemma III.3, $\partial_v f_4 < 0$. Thus the maximizer is on $v = 0$, which is edge CA

$$f_4(u, 0) = \frac{(10 - 2\sqrt{5})u + (5 + 2\sqrt{5})}{(5 - \sqrt{5})u + \sqrt{5}}.$$

Its derivative is

$$\frac{d}{du} f_4(u, 0) = \frac{5(\sqrt{5} - 5)}{\big((5 - \sqrt{5})u + \sqrt{5}\big)^2} < 0.$$

Therefore $f_4(u, 0)$ is strictly decreasing on $u \in [0, 1]$, and the maximum on the edge $v = 0$ is attained at $u = 0$.

(A) Maximizers in T_1. Maximizing f_1 and f_6 in T_1 was already done in the case $m = 3, 4$, so we skip them.

For f_3, from Lemma III.3, $\partial_v f_3 < 0$. Thus the maximizer is on $v = 0$, which is edge CA. Along this edge,

$$f_3(u, 0) = \frac{(10 - 2\sqrt{5})u + (5 + 2\sqrt{5})}{(5 - \sqrt{5})u + \sqrt{5}}.$$

Its derivative is

$$\frac{d}{du} f_3(u, 0) = \frac{5(\sqrt{5} - 5)}{\big((5 - \sqrt{5})u + \sqrt{5}\big)^2} < 0.$$

Therefore $f_3(u, 0)$ is strictly decreasing on $u \in [0, 1]$, and the maximum on the edge $v = 0$ is attained at $u = 0$.

(B) Maximizers in T_2. For f_1, both $\partial_u f_1$ and $\partial_v f_1$ are strictly positive. Evaluating f_1 along edge $L_{1,3}$ shows that

$$f_1\Big(u, \frac{10 + 2\sqrt{5} - 2(5 + \sqrt{5})\,u}{5 + 7\sqrt{5}}\Big) = \frac{(-10 + 10\sqrt{5})\,u + (25 + 11\sqrt{5})}{(-10 + 2\sqrt{5})\,u + (15 + 5\sqrt{5})}.$$

Its derivative is

$$\frac{d}{du} f_1(u, v(u)) = \frac{240 + 160\sqrt{5}}{\big((-10 + 2\sqrt{5})\,u + (15 + 5\sqrt{5})\big)^2} > 0.$$

Therefore, the maximum is attained at the endpoint with the largest u, i.e., at the vertex A.

For f_3, we have $\partial_v f_3 < 0$. Hence any maximizer must lie on $CA \cap T_2$ or on $L_{1,6}$. From the previous calculation, along CA we also have $\partial_u f_3 < 0$. Therefore, if the maximizer lies on $CA \cap T_2$, it must occur at the endpoint where $CA \cap T_2$ meets $L_{1,6}$. Consequently, it suffices to restrict attention to $L_{1,6}$. Evaluating f_3 along edge $L_{1,6}$ shows that

$$f_3\Big(u, \frac{10 + 2\sqrt{5} - 12\sqrt{5}\,u}{7\sqrt{5} + 5}\Big) = \frac{(13 - 5\sqrt{5})u + (13 + 6\sqrt{5})}{(5 - 7\sqrt{5})u + (5 + 4\sqrt{5})}.$$

Its derivative is

$$\frac{d}{du} f_3 = \frac{110 + 88\sqrt{5}}{\big((5 - 7\sqrt{5})u + (5 + 4\sqrt{5})\big)^2} > 0.$$

Therefore the maximum of f_3 over $L_{1,6}$ is attained at the endpoint where $v = 0$, i.e.,

$$(u, v) = \Big(\frac{1 + \sqrt{5}}{6},\, 0\Big).$$

For f_6, both $\partial_u f_6$ and $\partial_v f_6$ are strictly negative. Thus the maximum is on edge $L_{1,6}$, which has already been calculated in the case $m = 3, 4$.

(C) Maximizers in T_3. The maximizer for f_1 in T_3 is on edge AB, and maximizing f_1 along AB was already done in the case $m = 3, 4$.

For f_3, since $\partial_v f_3 < 0$, the maximizer is on edge $L_{1,3}$. Since on that edge, $f_1 = f_3$, it is equivalent to evaluating f_1 along $L_{1,3}$, which was already done above.

For f_6, since $\partial_v f_6 < 0$, the maximizer is on edge $L_{1,3}$.

$$f_6\Big(u, \frac{10 + 2\sqrt{5} - 2(5 + \sqrt{5})\,u}{5 + 7\sqrt{5}}\Big) = \frac{(10\sqrt{5} - 10)\,u + (25 + 11\sqrt{5})}{20u + (15 + 5\sqrt{5})}.$$

Differentiating gives

$$\frac{d}{du} f_6 = -\frac{40(10 + 3\sqrt{5})}{\big(20u + (15 + 5\sqrt{5})\big)^2} < 0.$$

Therefore, the maximum of f_6 over $L_{1,3}$ is attained at $u = 0$, i.e.,

$$(u, v) = \Big(0,\ \frac{1 + 3\sqrt{5}}{11}\Big).$$

Case $m = 7$ (the denominator is in $\{\boldsymbol{g}_7, \boldsymbol{g}_9\}$).

The switching condition $|\boldsymbol{x} \cdot \boldsymbol{g}_7| = |\boldsymbol{x} \cdot \boldsymbol{g}_9|$ splits into

$$L^+_{7,9}:\ \boldsymbol{x} \cdot \boldsymbol{g}_7 = \boldsymbol{x} \cdot \boldsymbol{g}_9, \qquad L^-_{7,9}:\ \boldsymbol{x} \cdot \boldsymbol{g}_7 = -\boldsymbol{x} \cdot \boldsymbol{g}_9,$$

which reduce to

$$L^+_{7,9}:\ v = -2u, \qquad L^-_{7,9}:\ v = (2\sqrt{5} - 4)(1 - u).$$

The switching line $L^+_{7,9}:\ v = -2u$ intersects T' only at the vertex $C = (0, 0)$. Hence, it suffices to consider the two subregions partitioned by

$$L^-_{7,9}:\ v = (2\sqrt{5} - 4)(1 - u).$$

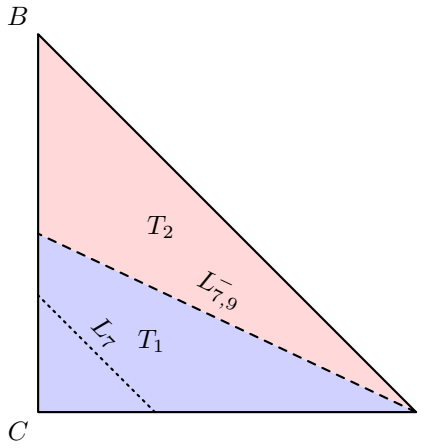

Fig. 4: Triangle T' in (u, v)-coordinates, the switching line $L_{7,9}^-$, and the zero line $L_7 : \ x \cdot g_7 = 0$.

We further denote by L_7 the zero line of $\boldsymbol{x}\cdot\boldsymbol{g}_7$, i.e., $\boldsymbol{x}\cdot\boldsymbol{g}_7 = 0$.

In subregion T_1, the ordering satisfies

$$|\boldsymbol{x} \cdot \boldsymbol{g}_9| \geq |\boldsymbol{x} \cdot \boldsymbol{g}_7|.$$

Moreover, since $\boldsymbol{x} \cdot \boldsymbol{g}_9 \geq 0$ throughout T', the m-height function for $m = 7$ reduces to

$$f_9(u, v) = \frac{\boldsymbol{x} \cdot \boldsymbol{g}_0}{\boldsymbol{x} \cdot \boldsymbol{g}_9}.$$

By Lemma III.3, we have

$$\partial_u f_9 < 0, \qquad \partial_v f_9 > 0 \quad \text{on } T'.$$

Therefore, the maximum of f_9 over T_1 is attained at the vertex with minimal u and maximal v, namely at the intersection of $L_{7,9}^-$ and the edge BC, which is

$$(u, v) = (0,\ 2\sqrt{5} - 4).$$

In subregion T_2, the ordering is reversed and the m-height function is

$$f_7(u, v) = \frac{\boldsymbol{x} \cdot \boldsymbol{g}_0}{-\boldsymbol{x} \cdot \boldsymbol{g}_7}.$$

Then direct differentiation yields

$$\partial_u f_7 = \frac{\left(1 - \frac{\sqrt{5}}{5}\right)v - (1 + \sqrt{5})}{D(u, v)^2} < 0,$$
$$\partial_v f_7 = \frac{\left(\frac{\sqrt{5}}{5} - 1\right)u - \left(\frac{3}{2} + \frac{7\sqrt{5}}{10}\right)}{D(u, v)^2} < 0.$$

Hence f_7 is strictly decreasing in both variables, and its maximum over T_2 must be attained on the boundary $L_{7,9}^-$.

Evaluating f_7 along $L_{7,9}^- : \ v = (2\sqrt{5} - 4)(1 - u)$ gives

$$f_7\Big(u,\ (2\sqrt{5} - 4)(1 - u)\Big) = \frac{(3 - \sqrt{5})u + \sqrt{5}}{(3 - \sqrt{5})u + (\sqrt{5} - 2)}.$$

Differentiating,

$$\frac{d}{du} f_7\Big(u,\ (2\sqrt{5} - 4)(1 - u)\Big) = \frac{2(\sqrt{5} - 3)}{\big((3 - \sqrt{5})u + (\sqrt{5} - 2)\big)^2} < 0.$$

so this restriction is strictly decreasing in u. Consequently, the maximum of f_7 on T_2 is attained at the endpoint $u = 0$, i.e.,

$$(u, v) = (0,\ 2\sqrt{5} - 4).$$

This completes the proof. □

IV. Frame-theoretic codes: Motivations

The dodecahedral code is a special frame-theoretic code: it is an OSPC code, namely, the columns of its generator matrix (and of its parity-check matrix) form a unit-norm tight frame (UNTF). In the following, we explore more general frame-theoretic constructions for Analog ECCs. For such frame-theoretic codes, their *coherence* can play an important role in controlling the m-heights of Analog ECCs, as the following analysis shows.

Let $G = [\boldsymbol{g}_0, \ldots, \boldsymbol{g}_{n-1}] \in \mathbb{R}^{k\times n}$ be a matrix whose columns form a unit-norm frame in $\mathbb{R}^k$, and let $M = G^\top G$ be the corresponding Gram matrix. The coherence of G is defined as

$$\mu(G) := \max_{0\leq i\neq j\leq n-1} |M_{ij}|.$$

The coherence is the largest absolute inner product between two distinct columns.

For any unit-norm frame of n vectors in $\mathbb{R}^k$, the Welch bound [12] gives the universal lower bound

$$\mu(G) \geq \mu_{\text{Welch}}(n, k),$$

where $\mu_{\text{Welch}}(n, k) := \sqrt{\frac{n-k}{k(n-1)}}$. An equiangular tight frame (ETF) attains this lower bound, so its coherence satisfies

$$\mu(G) = \mu_{\text{Welch}}(n, k).$$

The next theorem shows how the coherence, tightness and unit-norm properties together control the m-height of the corresponding analog code. Specifically, the theorem provides an upper bound on the m-height of an $[n, k]$ OSPC code in terms of the coherence of an ortho-spherical generator matrix of the code. The theorem improves on Theorem 11 in [9], and, for a range of parameters, also on Theorem 13 therein.

Theorem IV.1. *Let $\mathcal{C}$ be an $[n, k]$ OSPC code and let $G \in \mathbb{R}^{k\times n}$ be an ortho-spherical generator matrix of $\mathcal{C}$ with coherence $\mu = \mu(G)$. For any positive integer $m \leq \lceil((n/k) - 1)/\mu\rceil$, the m-height of $\mathcal{C}$ satisfies*

$$\frac{n}{k} - 1 - (m - 1)\mu > 0,$$

the m-height of $\mathcal{C}$ satisfies

$$h_m(\mathcal{C}) \leq \sqrt{\frac{n - m}{\frac{n}{k} - 1 - (m - 1)\mu}}.$$

In particular, if the columns of G form an ETF, then

$$h_m(\mathcal{C}) \leq \sqrt{\frac{k(n - m)\sqrt{n - 1}}{(n - k)\sqrt{n - 1} - (m - 1)\sqrt{(n - k)k}}}.$$

Proof. Because m-height does not depend on the scaling of the codeword, we can assume $\|\boldsymbol{u}\|_2 = 1$. Since G is a UNTF, $GG^\top = (n/k)I_k$. For $\boldsymbol{c} = \boldsymbol{u}G$, we then have

$$\|\boldsymbol{c}\|_2^2 = \boldsymbol{u}GG^\top\boldsymbol{u}^\top = \frac{n}{k}.$$

Let $T \subseteq [n\rangle$ be an index set of size m corresponding to $|c_{(0)}|, \ldots, |c_{(m-1)}|$. If ties occur, we choose any such T by breaking ties arbitrarily. Namely, T collects the indices of the largest m magnitudes of $\boldsymbol{c}$. Then every coordinate outside T has magnitude at most $|c_{(m)}|$, and hence

$$\frac{n}{k} = \|\boldsymbol{c}\|_2^2 \le \sum_{i\in T} |c_i|^2 + (n-m)|c_{(m)}|^2.$$

Let G_T denote the submatrix of G with columns indexed by T. By the min-max characterization of the largest singular value,

$$\sum_{i\in T} |c_i|^2 = \|\boldsymbol{u}G_T\|_2^2 \le \lambda_{\max}(G_T G_T^\top).$$

The nonzero eigenvalues of $G_T G_T^\top$ and $G_T^\top G_T$ are the same. Moreover, since the columns of G form a UNTF, the Gram matrix $G_T^\top G_T$ has diagonal entries equal to 1, and its off-diagonal entries have absolute value at most μ. By the Gershgorin circle theorem [14],

$$\lambda_{\max}(G_T G_T^\top) = \lambda_{\max}(G_T^\top G_T) \le 1 + (m-1)\mu.$$

Combining the above inequalities, we have

$$\frac{n}{k} \le 1 + (m-1)\mu + (n-m)|c_{(m)}|^2,$$
$$|c_{(m)}| \ge \sqrt{\frac{\frac{n}{k} - 1 - (m-1)\mu}{n-m}}.$$

Since $\|\boldsymbol{u}\|_2 = 1$ and the columns of G have unit norm, $|c_{(0)}| \le 1$. Therefore,

$$h_m(\mathcal{C}) = \max_{\boldsymbol{c}\in\mathcal{C}\setminus\{\boldsymbol{0}\}} \frac{|c_{(0)}|}{|c_{(m)}|} \le \max_{\boldsymbol{c}\in\mathcal{C}\setminus\{\boldsymbol{0}\}} \frac{1}{|c_{(m)}|}$$
$$\le \sqrt{\frac{n-m}{\frac{n}{k} - 1 - (m-1)\mu}}.$$

The hypothesis $\frac{n}{k} - 1 - (m-1)\mu > 0$ ensures that the denominator is positive. This proves the result. □

When $m > 1$, the upper bound of Theorem IV.1 is increasing in μ, thereby motivating us to look for constructions where μ is small. However, the lower bound $\mu_{\text{Welch}}(n,k)$ is achieved only by ETFs, which are not known to exist for all (n,k) pairs. Therefore we shall explore *incoherent tight frames* (ITFs), which are tight frames whose coherence is not necessarily minimized.

V. Analog ECC Construction via Incoherent Tight Frames

We now describe a construction method for analog codes based on ITFs. The method follows the alternating-projection framework of Tropp *et al.* [13]. To optimize the generator matrix G of an $[n,k]$ Analog ECC, the method optimizes its Gram matrix $M = G^\top G$. Specifically, the unit-norm property, coherence, and tightness of G are then determined, respectively, by the diagonal entries,off-diagonal entries, and eigenvalues of M.

A. Design objective and feasibility formulation

For a general (n,k) pair, our objective of design is to seek a matrix $G \in \mathbb{R}^{k\times n}$ that retains the following features:

(i) Tightness condition: $GG^\top = \frac{n}{k} I_k$, which means that the columns of G form a tight frame in $\mathbb{R}^k$,
(ii) Coherence condition: $\mu(G)$ is small (ideally close to the Welch bound),
(iii) Unit-norm condition: $\|\boldsymbol{g}_i\|_2$ is close to 1 for all columns $\boldsymbol{g}_i$ of G.

Let $M = G^\top G$ be the Gram matrix. The tightness condition $GG^\top = \frac{n}{k} I_k$ implies on M the following spectral constraint: k eigenvalues of M are n/k, and the remaining $n-k$ eigenvalues are 0. The coherence condition becomes $\mu(G) = \max_{i\neq j} |M_{ij}|$. The unit-norm condition becomes $M_{ii} = 1\ \forall i$.

Let $\mathbb{S}^n$ denote the set of $n \times n$ real symmetric matrices. As in [13], for a target coherence cap $\alpha \ge \mu_{\text{Welch}}(n,k)$, define

$$\mathcal{B}(\alpha) := \left\{ M \in \mathbb{S}^n : \begin{array}{ll} M_{ii} = 1 & \forall i, \\ |M_{ij}| \le \alpha & \forall i \neq j \end{array} \right\},$$

let $\lambda_0(M) \ge \cdots \ge \lambda_{n-1}(M)$ denote the eigenvalues of M, and define

$$\mathcal{T}_k := \left\{ M \in \mathbb{S}^n : \begin{array}{r} \lambda_0(M) = \cdots = \lambda_{k-1}(M) = \frac{n}{k}, \\ \lambda_k(M) = \cdots = \lambda_{n-1}(M) = 0 \end{array} \right\}.$$

The set $\mathcal{B}(\alpha)$ enforces unit diagonal entries and bounds the off-diagonal entries, while $\mathcal{T}_k$ enforces the Gram-spectrum condition of a tight frame in $\mathbb{R}^k$. The construction can therefore be written as the problem of finding a Gram matrix such that $M \in \mathcal{B}(\alpha) \cap \mathcal{T}_k$. This feasibility constraint becomes more restrictive as α approaches the Welch bound.

B. Alternating-projection iteration for code construction

The algorithm constructs a sequence of Gram matrices $M^{(0)}, M^{(1)}, M^{(2)}, \ldots \in \mathbb{R}^{n\times n}$, by alternating between the two constraint sets $\mathcal{B}(\alpha)$ and $\mathcal{T}_k$. (Each iteration first projects the Gram matrix $M^{(i)}$ onto $\mathcal{B}(\alpha)$ and then onto $\mathcal{T}_k$ to get $M^{(i+1)}$.) As initialization, the algorithm starts with a random UNTF $G^{(0)} \in \mathbb{R}^{k\times n}$. Define $M^{(0)} := (G^{(0)})^\top G^{(0)} \in \mathbb{R}^{n\times n}$. This initial Gram matrix is symmetric (indeed, positive semidefinite). The algorithm then iterates with the following two steps:

Step 1: Projection onto $\mathcal{B}(\alpha)$. Given the current matrix $M^{(t)}$, define the projection $P_{\mathcal{B}(\alpha)}\big(M^{(t)}\big)$ entrywise by

$$\Big(P_{\mathcal{B}(\alpha)}\Big(M^{(t)}\Big)\Big)_{ij} = \begin{cases} 1, & i = j, \\ \mathrm{clip}\Big(M_{ij}^{(t)}, -\alpha, \alpha\Big), & i \neq j, \end{cases}$$

where $\mathrm{clip}(x, \ell, u) := \min\{u, \max\{\ell, x\}\}$. Set

$$\widetilde{M}^{(t)} := P_{\mathcal{B}(\alpha)}\Big(M^{(t)}\Big).$$

This step sets the diagonal entries to one and clips all off-diagonal entries into the interval $[-\alpha, \alpha]$. It therefore enforces the unit-norm and coherence conditions.

Step 2: Projection onto $\mathcal{T}_k$. To compute $P_{\mathcal{T}_k}\Big(\widetilde{M}^{(t)}\Big)$, take an eigen-decomposition

$$\widetilde{M}^{(t)} = V \Lambda V^\top, \qquad \lambda_0 \geq \lambda_1 \geq \cdots \geq \lambda_{n-1},$$

where λ_i are the eigenvalues of $\widetilde{M}^{(t)}$. Let $V_k \in \mathbb{R}^{n \times k}$ be the matrix of eigenvectors corresponding to k largest eigenvalues $\lambda_0, \ldots, \lambda_{k-1}$. Then the projection has the closed form

$$P_{\mathcal{T}_k}\Big(\widetilde{M}^{(t)}\Big) = \frac{n}{k} V_k V_k^\top.$$

Define

$$M^{(t+1)} := P_{\mathcal{T}_k}\Big(\widetilde{M}^{(t)}\Big).$$

Equivalently,

$$M^{(t+1)} = P_{\mathcal{T}_k}\Big(P_{\mathcal{B}(\alpha)}\Big(M^{(t)}\Big)\Big).$$

This step maintains a rank-k positive semidefinite Gram matrix that satisfies the tightness condition.

After a preset number T of iterations (e.g., $T = 1000$), the algorithm computes a $k \times n$ matrix G as follows: let V_k be the matrix of eigenvectors, where the corresponding eigenvalue is n/k in the eigen-decomposition of $M^{(T)}$ and let

$$G := \sqrt{\frac{n}{k}}\, V_k^\top \in \mathbb{R}^{k \times n}.$$

If $M^{(T)} \in \mathcal{B}(\alpha) \cap \mathcal{T}_k$, then the matrix G is a UNTF with coherence at most α. G is tight by construction, while the unit-norm and coherence constraints are approximated by how closely the final iterate satisfies $\mathcal{B}(\alpha)$.

VI. Results on m-heights of concrete codes

This section summarizes the m-height values obtained by the concrete code constructions in this paper. Table I gives a compact comparison with previously reported values, while Table II provides broader results for the frame construction method. Across these tables, the main pattern is consistent: highly symmetric codes give strong benchmark examples, and incoherent frame constructions can extend this behavior to a wider range of parameter pairs.

A. Overall comparison with best known and structured codes

We summarize the m-height values obtained by the concrete codes constructed in this paper in Table I, which also presents a comparison with previously known m-heights. Here $h_m^\star$ denotes the best known m-height reported in previous works. Most of these values are taken from [10], while the entries for $(n, k, m) = (10, 3, 4)$ and $(10, 3, 5)$ are taken from [11]. h_m^{Geo} denotes the m-height of codes whose generator matrices are obtained from geometric constructions. More specifically, for $(n, k) = (6, 2)$, this is the polygonal construction, which is the same as the code $\mathcal{C}_{\mathrm{poly}}^\perp(n)$ in Example 4 of [11]. For $(n, k) = (6, 3)$ and $(10, 3)$, it corresponds to $\mathcal{C}_{\mathrm{ico}}^\perp$ and $\mathcal{C}_{\mathrm{dod}}^\perp$ in Examples 5 and 6 of [11], respectively. And h_m^{ITF} denotes the m-height of codes constructed using the ITF algorithm in Section V. The incoherent tight frame construction is not included for $k = 2$.

The comparison shows that the geometric constructions already provide strong m-height values for several parameter settings. The $(6, 2)$ code improves the previous value for $m = 3$, and the $(6, 3)$ code improves the known values for both $m = 2$ and $m = 3$. For the dodecahedral case, the $(10, 3)$ code improves the known values for $m = 3$, $m = 6$, and $m = 7$. These examples show that exact geometric symmetry can lead to strong analog ECCs. At the same time, Table I also shows the limitation of exact constructions, since they cover only a small number of parameter pairs. This motivates the broader frame construction results in the next subsection.

TABLE I: m-heights of analog ECCs. (Here red values indicate the smallest m-heights for given (n, k, m) parameters, while "/" means "not applicable".)

n	k	m	$h_m^\star$	h_m^{Geo}	h_m^{ITF}
6	2	3	2.28	2	/
6	3	2	2.87	2.24	2.24
6	3	3	7.00	4.24	4.24
10	3	2	1.00	1.62	1.60
10	3	3	2.12	1.76	2.00
10	3	4	2.55	3.00	2.35
10	3	5	2.96	4.24	2.69
10	3	6	17.18	4.24	7.00
10	3	7	69.44	9.47	∞
10	4	4	7.22	/	3.65
10	4	5	21.56	/	6.02
10	5	3	8.90	/	3.00
10	6	2	4.00	/	3.65
24	12	4	/	/	5.19
24	12	8	/	/	56.71

B. Analog ECCs via incoherent tight frame construction

Table II reports the m-height values obtained from the incoherent tight frame construction over a broader range of (n, k) pairs.

In Table II, h_m^{ITF} denotes the value obtained from the incoherent tight frame algorithm and $h_m^\star$ denotes the best value reported in previous works. The results show that: (1) This construction has discovered state-of-the-art codes whose m-heights are smaller than the best codes known so far in quite

TABLE II: m-heights of analog ECCs constructed using incoherent tight frame construction.

n	k	m	h_m^{ITF}	$h_m^\star$	n	k	m	h_m^{ITF}	$h_m^\star$
8†	3	5	9.097	20.37 [10]	15	5	7	7.348	/
9	3	3	2.121	3.05 [10]	15	6	3	3	/
9	3	4	2.414	5.76 [10]	15†	7	3	3.482	/
10†	3	4	2.353	2.55 [11]	15†	7	4	4.515	/
10†	3	5	2.688	2.96 [11]	15†	7	5	7.022	/
10	4	3	2.511	5 [10]	15†	8	2	3.706	/
10	4	5	6.023	21.56 [10]	15†	8	4	6.955	/
10*	5	3	3	8.90 [10]	15	9	2	4	/
11†	3	3	1.691	/	15	9	3	5	/
11†	3	4	2.338	/	16*	6	4	3	/
11†	5	2	2.582	/	16*	6	5	3	/
11†	5	4	5.366	/	16†	8	3	3.922	/
11†	6	2	3.098	/	16†	8	5	8.288	/
12†	3	3	1.615	/	16†	8	7	136.845	/
12	5	2	2.500	/	16*	10	2	5	/
12	5	3	3	/	16*	10	3	5	/
12	5	4	3	/	17†	4	7	2.959	/
12	7	3	5	/	17†	8	4	4.660	/
12	8	2	5	/	17†	9	3	4.413	/
12†	8	3	15.592	/	17†	9	4	7.051	/
13†	3	5	2.175	/	18	4	7	2.588	/
14†	4	6	3.256	/	18	4	8	2.993	/
14†	4	9	28.009	/	18	4	9	3.852	/
14*	7	3	3.605	/	18	4	11	9.027	/
14*	7	4	4.211	/	18†	6	3	2.687	/
14*	7	5	7.605	/	18†	7	4	3.513	/
14*	7	6	10.211	/	18†	8	3	3.560	/
14*	7	7	36.027	/	18†	8	7	20.786	/
14†	8	2	3.994	/	18*	9	2	3.795	/
14†	9	3	7.552	/	18*	9	3	3.980	/
14†	10	3	30.772	/	18*	9	4	4.123	/
15	5	3	2.469	/	18*	9	5	5.123	/
15	5	5	3.116	/	18	14	2	9.115	/
15	5	6	3.449	/					

$h_m^\star$ represents the m-height reported in previous works.
Each such $h_m^\star$ is followed by the citation of that previous work.
h_m^{ITF} denotes the m-height by the incoherent tight frame algorithm.
† Unit-norm column constraint not exactly satisfied.
* Frame construction achieves ETF exactly.

a few cases, as shown by the first eight rows of the left column of table II; (2) This construction has discovered new codes of small m-heights for numerous (n, k, m) parameters where no previous codes were known, as shown by the rest of table II. When the method is applied to $(n, k) = (6, 3)$, it converges exactly to $\mathcal{C}_{\mathrm{ico}}^{\perp}$, so the resulting value agrees with the geometric construction.

For the many codes constructed using the frame-theoretic approach, which are shown in the column named h_m^{ITF} of table II, they have been constructed with 3 sub-approaches: (1) Codes that are exact ETFs, which are marked by * in the table; (2) Codes that do not exactly satisfy the unit-norm condition of an ETF, which are marked by † in the table; (3) Codes that do not exactly satisfy the equiangular and tightness constraints of an ETF, which are neither marked by * nor by †. Both sub-approaches (2) and (3) are moderate relaxations of sub-approach (1), and they were taken because exact ETFs do not exist (or are hard to find) in many cases. Note that even for sub-approaches (2) and (3), the deviations from spherical codes are still small. For those codes, we calculate the ratio of the maximum and minimum column norms of the generator matrix of each code; then the maximum, average and variance of those ratios are 1.01737, 1.00076 and 5.31×10^{-6}, respectively, which are all small. We also observe that good m-height performance is often associated with coherence values close to the Welch bound. For the same table, the average ratio between coherence and the Welch bound is 1.259, the maximum ratio is 1.914, and the variance is 0.047. This is consistent with the frame theoretic motivation developed earlier in the paper.

The incoherent tight frame method also extends beyond the exact geometric cases. In our experiments, the number of iterations is set to 1000. The construction itself is efficient. For example, the running time is less than 1 second for $(64, 32)$ on a personal laptop and less than 1 minute for $(128, 64)$. The main computational bottleneck is not the frame search, but the evaluation of m-height, since the currently available methods become difficult for long codes [10], [11]. In addition, the tightness constraint can be restrictive, so the method does not guarantee a finite m-height for every output. Still, the results in Table II show that this approach is a practical way to construct competitive analog ECCs.

REFERENCES

[1] A. Sebastian, M. Le Gallo, R. Khaddam-Aljameh, and E. Eleftheriou, "Memory devices and applications for in-memory computing," *Nature Nanotechnol.*, vol. 15, no. 7, pp. 529–544, 2020.

[2] W. Wang et al., "A memristive deep belief neural network based on silicon synapses," *Nature Electron.*, vol. 5, no. 12, pp. 870–880, Dec. 2022.

[3] H.-S.-P. Wong and S. Salahuddin, "Memory leads the way to better computing," *Nature Nanotechnol.*, vol. 10, no. 3, pp. 191–194, Mar. 2015.

[4] M. Le Gallo et al., "A 64-core mixed-signal in-memory compute chip based on phase-change memory for deep neural network inference," *Nature Electron.*, vol. 6, no. 9, pp. 680–693, Aug. 2023.

[5] W. Zhang et al., "Edge learning using a fully integrated neuro-inspired memristor chip," *Science*, vol. 381, no. 6663, pp. 1205–1211, Sep. 2023.

[6] R. M. Roth, "Fault-tolerant neuromorphic computing on nanoscale crossbar architectures," in *Proc. IEEE Inf. Theory Workshop (ITW)*, Nov. 2022, pp. 202–207.

[7] R. M. Roth, "Analog error-correcting codes," *IEEE Trans. Inf. Theory*, vol. 66, no. 7, pp. 4075–4088, Jul. 2020.

[8] R. M. Roth, "Corrections to Analog error-correcting codes," *IEEE Trans. Inf. Theory*, vol. 69, no. 6, pp. 3793–3794, Jun. 2023.

[9] H. Wei and R. M. Roth, "Multiple-error-correcting codes for analog computing on resistive crossbars," *IEEE Trans. Inf. Theory*, vol. 70, no. 12, pp. 8647–8658, Aug. 2024.

[10] A. Jiang, "Analog error-correcting codes: designs and analysis," *IEEE Trans. Inf. Theory*, vol. 70, no. 11, pp. 7740–7756, Nov. 2024.

[11] R. M. Roth, Z. Zhu, C. Yuan, P. H. Siegel, and A. Jiang, "On the height profile of analog error-correcting codes," arXiv:2602.20366 [cs.IT], 2026.

[12] S. F. D. Waldron, *An Introduction to Finite Tight Frames*. New York, NY, USA: Birkhäuser, 2018.

[13] J. A. Tropp, I. S. Dhillon, R. W. Heath, and T. Strohmer, "Designing structured tight frames via an alternating projection method," *IEEE Trans. Inf. Theory*, vol. 51, no. 1, pp. 188–209, Jan. 2005.

[14] G. Strang, *Introduction to Linear Algebra*, 5th ed. Wellesley, MA, USA: Wellesley-Cambridge Press, 2016.